arXiv:hep-ph/0208237v2 27 Sep 2002

# Deep inelastic $J/\Psi$ production at HERA in the colour singlet model with $k_T$-factorization

A.V. Lipatov [1)]
*Physical Department, M.V. Lomonosov Moscow State University, 119992 Moscow, Russia*

N.P. Zotov [2)]
*D.V. Skobeltsyn Institute of Nuclear Physics, M.V. Lomonosov Moscow State University, 119992 Moscow, Russia*

## Abstract

We consider $J/\Psi$ meson production in $ep$ deep inelastic scattering in the colour singlet model using the $k_T$-factorization QCD approach. We investigate the $z$-, $Q^2$-, $\mathbf{p}_T^2$-, $y^*$- and $W$-dependences of inelastic $J/\Psi$ production on different forms of the unintegrated gluon distribution. The $\mathbf{p}_T^2$- and $Q^2$-dependences of the $J/\Psi$ spin aligment parameter $\alpha$ are presented also. We compare the theoretical results with recent experimental data taken by the H1 and ZEUS collaborations at HERA. It is shown that experimental study of the polarization $J/\Psi$ mesons at $Q^2 < 1\,\mathrm{GeV}^2$ is an additional test of BFKL gluon dynamics.

[1)] E-mail: artem_lipatov@mail.ru
[2)] E-mail: zotov@theory.sinp.msu.ru

# 1 Introduction

It is known that from heavy quark and quarkonium production processes one can obtain unique information on gluon structure function of the proton because of the dominance of the photon-gluon or gluon-gluon fusion subprocess in the framework of QCD [1–4]. Studying of gluon distributions at modern collider energy (such as HERA, Tevatron) is important for prediction of heavy quark and quarkonium production cross sections at future colliders (LHC, THERA). At the energies of HERA and LEP/LHC colliders heavy quark and quarkonium production processes are so called semihard processes [5]. In such processes by definition the hard scattering scale $\mu \sim m_Q$ is large compare to the $\Lambda_{\rm QCD}$ parameter but on the other hand $\mu$ is much less than the total center-of-mass energy: $\Lambda_{\rm QCD} \ll \mu \ll \sqrt{s}$. The last condition implies that the processes occur in small $x$ region: $x \simeq m_Q/\sqrt{s} \ll 1$, and that the cross sections of heavy quark and quarkonium production processes are determined by the behavior of gluon distributions in the small $x$ region.

It is also known that in the small $x$ region the standard parton model (SPM) assumptions about factorization of gluon distribution functions and subprocess cross sections are broken because the subprocess cross sections and gluon structure functions depend on a gluon transverse momentum $k_T$ [6–8]. So calculations of heavy quark production cross sections at HERA, Tevatron, LHC and other collider conditions are necessary to carry out in the so called $k_T$-factorization (or semihard) QCD approach, which is more preferable for small region than SPM.

The $k_T$-factorization QCD approach is based on Balitsky, Fadin, Kuraev, Lipatov (BFKL) [9] evolution equations. The resummation of the terms $\alpha_S^n \ln^n(\mu^2/\Lambda^2_{\rm QCD})$, $\alpha_S^n \ln^n(\mu^2/\Lambda^2_{\rm QCD}) \ln^n(1/x)$ and $\alpha_S^n \ln^n(1/x)$ in the $k_T$-factorization approach leads to the unintegrated (depends from $\mathbf{q}_T$) gluon distribution $\Phi(x, \mathbf{q}_T^2, \mu^2)$ which determine the probability to find a gluon carrying the longitudinal momentum fraction $x$ and transverse momentum $\mathbf{q}_T$ at probing scale $\mu^2$. The unintegrated gluon distribution reduce to the conventional gluon distribution $xG(x, \mu^2)$ once the $\mathbf{q}_T$ dependence is integrated out:

$$xG(x, \mu^2) = xG(x, Q_0^2) + \int\limits_{Q_0^2}^{\mu^2} \Phi(x, \mathbf{q}_T^2, \mu^2)\, d\mathbf{q}_T^2. \tag{1}$$

To calculate the cross section of a physical process the unintegrated gluon distributions have to be convoluted with off mass shell matrix elements corresponding to the relevant partonic subprocesses [6–8]. In the off mass shell matrix element the virtual gluon polarization tensor is taken in the BFKL form [5]:

$$L^{\mu\,\nu}(q) = \frac{q_T^\mu\, q_T^\nu}{\mathbf{q}_T^2}. \tag{2}$$

Nowadays, the significance of the $k_T$-factorization QCD approach becomes more and more commonly recognized [10]. It is already was used for the description of a wide class heavy quark and quarkonium production processes [6, 11–25], in particular, for the description heavy quark [6, 11, 14, 16, 20–23] and quarkonium [13, 15, 19, 24, 25] photo and leptoproduction. It is notable that calculations in $k_T$-factorization QCD approach results to some effects which are absent in other approaches. It is a more fast growth of total cross sections in comparison with SPM, a broadering of the $p_T$ spectra due to extra transverse momentum

of the colliding partons and other polarization properties of final particles in comparison with SPM.

We point out that heavy quark and quarkonium cross section calculations within the SPM in the fixed order of pQCD have some problems. For example, the very large discrepancy (by more than an order of magnitude) [26, 27] between the pQCD predictions for hadroproduction $J/\Psi$ and $\Upsilon$ mesons and experimental data at Tevatron was found. This fact has resulted in intensive theoretical investigations of such processes. In particular, it was required to enter additional transition mechanism from $c\bar{c}$-pair to the $J/\Psi$ mesons, so-called the colour octet (CO) model [28], where $c\bar{c}$-pair is produced in the color octet state and transforms into final colour singlet (CS) state by help soft gluon radiation. The CO model was supposed to be applicable to heavy quarkonium hadro and electroproduction processes. However, the contributions from the CO mechanism to the $J/\Psi$ meson photoproduction contradict the experimental data at HERA for $z$-distribution [29–32].

Another difficulty of the CO model is $J/\Psi$ polarization properties in $p\bar{p}$-interactions at Tevatron. In the framework of the CO model $J/\Psi$ mesons should be transverse polarized at the large transverse momenta $\mathbf{p}_T$. However, this fact contradicts the experimental data too.

The CO model has been applied earlier in analysis of the $J/\Psi$ inelastic production experimental data at HERA [33, 34]. However, this results are not agree with each other [34]. It is notable that results obtained within the usual collinear approach and CS model [35–38] underestimate experimental data by factor about 2.

Recently the first attempts to investigate a $J/\Psi$ polarization problem in $p\bar{p}$-interactions at Tevatron in $k_T$-factorization approach were made [24, 39, 40]. Also the theoretical prediction within semihard QCD approach [19] are stimulated the experimental analysis $J/\Psi$ polarization properties at HERA conditions. However the further theoretical and experimental studies of this problem are necessary.

Based on the above mentioned results we consider here the deep inelastic $J/\Psi$ production at HERA in the framework of the CS model and the $k_T$-factorization approach with emphasis of a role of a proton gluon distribution function. Using the CS model and formalism of the projection operator [41], we investigate the $Q^2$-, $\mathbf{p}_T^2$-, $z$-, $y^*$- and $W$-dependences of $J/\Psi$ production on different forms of the unintegrated gluon distribution. Special attention is given to the unintegrated gluon distributions obtained from BFKL evolution equation which has been applied earlier in our previous papers [15–18]. For studying $J/\Psi$ meson polarization properties we calculate the $\mathbf{p}_T^2$- and $Q^2$-dependences of the spin aligment parameter $\alpha$.

The outline of this paper is as follows. In Section 2 we give the formulas for the inelastic $J/\Psi$ electroproduction differential cross section in the $k_T$-factorization QCD approach. In Section 3 we describe the unintegrated gluon distributions which we use in our calculations. In Section 4 we give the formulas for $J/\Psi$ electroproduction off mass shell matrix elements in the CS model. In Section 5 we present the results of our calculations. Finally, in Section 6, we give some conclusions.

## 2 Deep inelastic $J/\Psi$ electroproduction cross section in the $k_T$-factorization QCD approach

In this section we calculate total and differential cross section for inelastic $J/\Psi$ electroproduction via the photon-gluon fusion QCD subprocess (Fig. 1) in the $k_T$-factorization QCD

approach. Let us define Sudakov variables of the process $e\,p \to e'\,J/\Psi\,X$:

$$\begin{aligned} p_{J/\Psi} = \alpha_1 p_e + \beta_1 p_p + p_{J/\Psi\,T}, \qquad p_g = \alpha_2 p_e + \beta_2 p_p + p_{g\,T}, \\ q_1 = x_1 p_e + q_{1T}, \qquad q_2 = x_2 p_p + q_{2T}, \end{aligned} \tag{3}$$

where

$$p_{J/\Psi}^2 = m_{J/\Psi}^2, \quad p_g^2 = 0, \quad q_1^2 = q_{1T}^2 = -Q^2, \quad q_2^2 = q_{2T}^2, \tag{4}$$

$p_{J/\Psi}$ and $p_g$ are 4-momenta of the $J/\Psi$ meson and final real gluon, $q_1$ and $q_2$ are 4-momenta of the initial virtual photon and gluon, $p_{J/\Psi\,T}$, $p_{g\,T}$, $q_{1\,T}$, $q_{2\,T}$ are transverse 4-momenta of these. In the center-of-mass frame of colliding particles we can write:

$$p_e = (E,\, 0,\, 0,\, E), \qquad p_p = (E,\, 0,\, 0,\, -E), \tag{5}$$

where

$$E = \frac{\sqrt{s}}{2}, \qquad p_e^2 = p_p^2 = 0, \qquad (p_e \cdot p_p) = \frac{s}{2}. \tag{6}$$

Sudakov variables are expressed as follows:

$$\begin{aligned} \alpha_1 = \frac{m_{J/\Psi\,T}}{\sqrt{s}} \exp(y_{J/\Psi}), \qquad \alpha_2 = \frac{\mathbf{p}_{g\,T}}{\sqrt{s}} \exp(y_g), \\ \beta_1 = \frac{m_{J/\Psi\,T}}{\sqrt{s}} \exp(-y_{J/\Psi}), \qquad \beta_2 = \frac{\mathbf{p}_{g\,T}}{\sqrt{s}} \exp(-y_g), \end{aligned} \tag{7}$$

where $m_{J/\Psi\,T}^2 = m_{J/\Psi}^2 + \mathbf{p}_{J/\Psi\,T}^2$, $m_{J/\Psi}$ is $J/\Psi$ meson mass, $y_{J/\Psi}$ and $y_g$ are c.m. rapidities of $J/\Psi$ meson and final gluon respectively. The inelastic $J/\Psi$ electroproduction differential cross section has the following form:

$$d\sigma(e\,p \to e'\,J/\Psi\,X) = \frac{dx_2}{x_2}\,\Phi(x_2,\,\mathbf{q}_{2T}^2,\,\mu^2)\,\frac{d\phi_2}{2\pi}\,d\mathbf{q}_{2T}^2\,d\hat{\sigma}(e\,g^* \to e'\,J/\Psi\,g'), \tag{8}$$

where $\phi_2$ is initial BFKL gluon azimuthal angle, $\Phi(x_2, \mathbf{q}_{2T}^2, \mu^2)$ is an unintegrated gluon distribution in the proton, and

$$\begin{aligned} d\hat{\sigma}(e\,g^* \to e'\,J/\Psi\,g') = \frac{(2\pi)^4}{2x_2 s}\,\sum |M|^2_{\rm SHA}(e\,g^* \to e'\,J/\Psi\,g') \times \\ \times \frac{d^3p'_e}{(2\pi)^3\,2p'^0_e}\,\frac{d^3p_{J/\Psi}}{(2\pi)^3\,2p^0_{J/\Psi}}\,\frac{d^3p_g}{(2\pi)^3\,2p^0_g}\,\delta^{(4)}(p_e + q_2 - p'_e - p_{J/\Psi} - p_g), \end{aligned} \tag{9}$$

where $\sum |M|^2_{\rm SHA}(e\,g^* \to e'\,J/\Psi\,g')$ is the off mass shell matrix element. In (9) $\sum$ indicates an averaging over initial particles polarization and a sum over polarization of final ones.

From (8) and (9) we obtain the following formula for the inelastic $J/\Psi$ electroproduction differential cross section in the $k_T$-factorization QCD approach:

$$\begin{aligned} d\sigma(e\,p \to e'\,J/\Psi\,X) = \frac{1}{128\pi^3}\,\frac{\Phi(x_2,\,\mathbf{q}_{2T}^2,\,\mu^2)}{(x_2\,s)^2\,(1-x_1)}\,\frac{dz}{z\,(1-z)}\,dy_{J/\Psi} \times \\ \times \sum |M|^2_{\rm SHA}(e\,g^* \to e'\,J/\Psi\,g')\,d\mathbf{p}_{J/\Psi\,T}^2\,dQ^2\,d\mathbf{q}_{2T}^2\,\frac{d\phi_1}{2\pi}\,\frac{d\phi_2}{2\pi}\,\frac{d\phi_{J/\Psi}}{2\pi}, \end{aligned} \tag{10}$$

where

$$x_1 = \alpha_1 + \alpha_2, \qquad x_2 = \beta_1 + \beta_2, \qquad \mathbf{q}_{1T} + \mathbf{q}_{2T} = \mathbf{p}_{J/\Psi\,T} + \mathbf{p}_{g\,T}, \tag{11}$$

$\phi_1$ and $\phi_{J/\Psi}$ are initial virtual photon and outgoing $J/\Psi$ meson azimuthal angles, $z = (p_{J/\Psi} \cdot p_p)/(q_1 \cdot p_p)$. If we take the limit $\mathbf{q}_{2T}^2 \to 0$ and if we average (10) over the transverse directions of the vector $\mathbf{q}_{2T}$, we obtain the formula for the differential cross section in the SPM:

$$d\sigma(e\,p \to e'\,J/\Psi\,X) = \frac{1}{128\pi^3}\,\frac{1}{(x_2\,s)^2\,(1-x_1)}\,\frac{dz}{z\,(1-z)}\,x_2 G(x_2,\,\mu^2)\times \\ \times \sum |M|^2_{\rm PM}(e\,g \to e'\,J/\Psi\,g')\,dy_{J/\Psi}\,d\mathbf{p}^2_{J/\Psi\,T}\,dQ^2\,\frac{d\phi_1}{2\pi}\,\frac{d\phi_{J/\Psi}}{2\pi}, \tag{12}$$

where $\sum |M|^2_{\rm PM}(e\,g \to e'\,J/\Psi\,g')$ is the matrix element in the SPM. Here $\sum$ indicates an averaging over initial particles polarization and a sum over polarization of final ones. We average over the transverse directions of the vector $\mathbf{q}_{2T}$ using the following expression:

$$\int d\mathbf{q}^2_{2T}\,\int \frac{d\phi_2}{2\pi}\,\Phi(x_2,\,\mathbf{q}^2_{2T},\,\mu^2)\,\sum |M|^2_{\rm SHA}(e\,g^* \to e'\,J/\Psi\,g') = \\ = x_2 G(x_2,\,\mu^2)\,\sum |M|^2_{\rm PM}(e\,g \to e'\,J/\Psi\,g'), \tag{13}$$

where

$$\int\limits_0^{2\pi} \frac{d\phi_2}{2\pi}\,\frac{q^\mu_{2T}\,q^\nu_{2T}}{\mathbf{q}^2_{2T}} = \frac{1}{2}\,g^{\mu\nu}. \tag{14}$$

## 3 Unintegrated gluon distributions

Various parametrizations of the unintegrated gluon distribution used in our calculations are discussed below.

We used the results of a BFKL-like parametrization of unintegrated gluon distribution (so called JB parametrization) according to the prescription given in [44]. The proposed method lies upon a straightforward perturbative solution of the BFKL equation where the collinear gluon density $xG(x,\mu^2)$ from the standard GRV set [45] is used as the boundary condition in the integral form (1). The unintegrated gluon density is calculated as a convolution of collinear gluon distribution $xG(x,\mu^2)$ with universal weight factors:

$$\Phi(x,\mathbf{q}_T^2,\mu^2) = \int\limits_x^1 \varphi(\eta,\mathbf{q}_T^2,\mu^2)\,\frac{x}{\eta}\,G\left(\frac{x}{\eta},\,\mu^2\right)\,d\eta, \tag{15}$$

where

$$\varphi(\eta,\mathbf{q}_T^2,\mu^2) = \begin{cases} \dfrac{\bar\alpha_S}{\eta\,\mathbf{q}_T^2} J_0\left(2\sqrt{\bar\alpha_S \ln(1/\eta)\ln(\mu^2/\mathbf{q}_T^2)}\right), & \text{if } \mathbf{q}_T^2 \le \mu^2, \\ \dfrac{\bar\alpha_S}{\eta\,\mathbf{q}_T^2} I_0\left(2\sqrt{\bar\alpha_S \ln(1/\eta)\ln(\mathbf{q}_T^2/\mu^2)}\right), & \text{if } \mathbf{q}_T^2 > \mu^2, \end{cases} \tag{16}$$

where $J_0$ and $I_0$ stand for Bessel function of real and imaginary arguments respectively, and $\bar\alpha_S = 3\alpha_S/\pi$. The parameter $\bar\alpha_S$ is connected with the Pomeron trajectory intercept: $\Delta = 4\bar\alpha_S \ln 2$ in the LO and $\Delta = 4\bar\alpha_S \ln 2 - N\bar\alpha_S^2$ in the NLO approximations, where $N \sim 18$ [46, 47]. The latter value of $\Delta$ have dramatic consequences for high energy phenomenology, however, some resummation procedures proposed in the last years lead to positive value of $\Delta \sim 0.2 - 0.3$ [47, 48]. Therefore in our calculations with (17) we used only the solution

of LO BFKL equation and considered $\Delta$ as a free parameter varying it from 0.166 to 0.53. Pomeron intercept parameter $\Delta = 0.35$ was obtained from the description of $p_T$ spectrum of $D^*$ meson electroproduction at HERA [20]. We used this value of the parameter $\Delta$ in present paper.

Then we use another set (the KMS parametrization) [49] is obtained from a unified BFKL and DGLAP description of $F_2$ data and includes the so called consistency constraint [50]. The consistency constraint introduce a large correction to the LO BFKL equation: about 70 of the full NLO corrections to the BFKL exponent $\Delta$ are effectively included in this constraint, as is declared in [51].

Finally, the third unintegrated gluon function used here is one proposed by Golec-Biernat and Wusthoff (GBW) which takes into account gluon saturation effects and has been applied earlier in analysis of the inclusive and diffractive $ep$-scattering data [52, 53]. It has the following form:

$$\Phi(x, \mathbf{q}_T^2, \mu^2) = \frac{3\sigma_0}{4\pi^2} \frac{1}{\alpha_S} R_0^2(x)\, \mathbf{q}_T^2 \, \exp(-R_0^2(x)\, \mathbf{q}_T^2), \tag{17}$$

where

$$R_0^2(x) = \frac{1}{\mathrm{GeV}^2} \left(\frac{x}{x_0}\right)^{\lambda/2}. \tag{18}$$

and $\sigma_0 = 23.03\,\mathrm{mb}$, $\lambda = 0.288$, $x_0 = 3.04 \cdot 10^{-4}$.

In expression (1) the accounting of the contribution of the unintegrated gluon distribution to integral at low $\mathbf{q}_T^2$ region $0 < \mathbf{q}_T^2 < Q_0^2$ was done by the collinear gluon density $xG(x, Q_0^2)$, where $Q_0^2 = 1\,\mathrm{GeV}^2$ for all gluon distributions.

## 4 Off mass shell matrix element for $e\,g^* \to e'\,J/\Psi\,g'$ process

In this section we give the formulas for $J/\Psi$ electroproduction off mass shell matrix elements in the CS model. There are six Feynman diagrams (Fig. 2) which describe partonic process $\gamma\,g^* \to J/\Psi\,g'$ at the leading order in $\alpha_S$ and $\alpha$. In the framework of the CS model and nonrelativistic approximation the production of $J/\Psi$ meson is considered as the production of a quark-antiquark system in the colour singlet state with orbital momentum $L = 0$ and spin momentum $S = 1$. The binding energy and relative momentum of quarks in the $J/\Psi$ are neglected. Such a way $m_{J/\Psi} = 2\,m_c$, where $m_c$ is charm mass. Taking into account the formalism of the projection operator [41] the amplitude of the process $\gamma\,g^* \to J/\Psi\,g'$ may be obtained from the amplitude of the process $\gamma\,g^* \to c\bar{c}\,g'$ after replacement:

$$v(p_{\bar{c}})\,\bar{u}(p_c) \to \hat{J}(p_{J/\Psi}) = \frac{\Psi(0)}{2\sqrt{m_{J/\Psi}}}\,\hat{\epsilon}(p_{J/\Psi})\,(\hat{p}_{J/\Psi} + m_{J/\Psi})\,\frac{1}{\sqrt{3}}, \tag{19}$$

where $\hat{\epsilon}(p_{J/\Psi}) = \epsilon_\mu(p_{J/\Psi})\,\gamma^\mu$, $\epsilon(p_{J/\Psi})$ is a 4-vector of the $J/\Psi$ polarization, $1/\sqrt{3}$ is the color factor, $\Psi(0)$ is the nonrelativistic meson wave function at the origin. In according with the standard Feynman rules for QCD diagrams we have:

$$\begin{gathered} M = e_c\, g^2\, \epsilon_\mu(q_1)\, \epsilon_\sigma(q_2)\, \epsilon_\rho(p_g) \times \\ \times Sp\left[\hat{J}(p_{J/\Psi})\,\gamma^\mu\,\frac{\hat{p}_c - \hat{q}_1 + m_c}{(p_c - q_1)^2 - m_c^2}\,\gamma^\sigma\,\frac{-\hat{p}_c - \hat{p}_g + m_c}{(-p_c - p_g)^2 - m_c^2}\,\gamma^\rho\right] \end{gathered} \tag{20}$$

+ 5 permutations of all gauge bosons. Here $\epsilon_\mu(q_1)$, $\varepsilon_\mu(q_2)$ are polarization vectors of the initial photon and gluon respectively, $\epsilon_\mu(p_g)$ is a 4-vector of the final gluon polarization. The summation on the $J/\Psi$ meson and final gluon polarizations is carried out by covariant formulas:

$$\sum \epsilon^\mu(p_{J/\Psi})\epsilon^{*\,\nu}(p_{J/\Psi}) = -g^{\mu\nu} + \frac{p^\mu_{J/\Psi} p^\nu_{J/\Psi}}{m^2_{J/\Psi}}, \tag{21}$$

$$\sum \epsilon^\mu(p_g)\epsilon^{*\,\nu}(p_g) = -g^{\mu\nu}, \tag{22}$$

The initial BFKL gluon polarization tensor is taken in form (2). We substitute here the full lepton tensor for the photon polarization tensor (including also the photon propagator factor and photon-lepton coupling):

$$\sum \epsilon^\mu(q_1)\epsilon^{*\,\nu}(q_1) = 2\,\frac{e^2}{Q^2}\,\left(-g^{\mu\nu} + \frac{4p^\mu_e p^\nu_e}{Q^2}\right). \tag{23}$$

For studing $J/\Psi$ polarized production we introduce the 4-vector of the longitudinal polarization $\epsilon^\mu_L(p_{J/\Psi})$ as follows [54]:

$$\epsilon^\mu_L(p_{J/\Psi}) = \frac{(p_{J/\Psi}\cdot p_p)}{\sqrt{(p_{J/\Psi}\cdot p_p)^2 - m^2_{J/\Psi}\,s}}\left(\frac{p^\mu_{J/\Psi}}{m_{J/\Psi}} - \frac{m_{J/\Psi} p^\nu_p}{(p_{J/\Psi}\cdot p_p)}\right). \tag{24}$$

In the limit $s \gg m^2_{J/\Psi}$ the polarization 4-vector satisfies usual conditions: $(\epsilon_L\cdot\epsilon_L) = -1$ and $(\epsilon_L\cdot p_{J/\Psi}) = 0$. The calculation of $\sum |M|^2_{\rm SHA}(e\,g^* \to e'\,J/\Psi\,g')$ and $\sum |M|^2_{\rm PM}(e\,g \to e'\,J/\Psi\,g')$ was done analitically by REDUCE system.

## 5 Numerical results and discussion

In this section we present the theoretical results in comparison with available experimental data taken by the H1 [42] and ZEUS [43] collaborations at HERA. There are three parameters which determine the common normalization factor of the cross section under consideration: $J/\Psi$ meson wave function at the origin $\Psi(0)$, charmed quark mass $m_c$ and factorization scale $\mu$. The value of the $J/\Psi$ meson wave function at the origin may be calculated in a potential model or obtained from the well known experimental decay width $\Gamma(J/\Psi \to \mu^+\mu^-)$. In our calculation we used the following choice $|\Psi(0)|^2 = 0.0876\,{\rm GeV}^3$ as in [55]. Concerning a charmed quark mass, the situation is not clear: on the one hand, in the nonrelativistic approximation one has $m_c = m_{J/\Psi}/2 = 1.55\,{\rm GeV}$, but on the other hand there are many examples when smaller value of a charm mass is used, for example, $m_c = 1.4\,{\rm GeV}$ [34, 56, 57]. In the present paper we used both of charm mass values. Also the most significant theoretical uncertanties refer to the choice of the factorization scale $\mu_F$ and renormalization one $\mu_R$. One of them is related to the evolution of the gluon distributions $\Phi(x, \mathbf{q}^2_T, \mu^2_F)$, the other is responsible for strong coupling constant $\alpha_S(\mu^2_R)$. As is often done in literature for simplicity we set them equal: $\mu_F = \mu_R = \mu$. In the present paper we used the following choice $\mu^2 = \mathbf{q}^2_{2T}$ as in [58].[3)]

The calculations of the inelastic $J/\Psi$ production cross section in the $k_T$-factorization approach have been made according to (10) and in the SPM — according to (12). The

[3)] The our preliminary results at [59] were obtained with $\mu^2 = m^2_{J/\Psi} + \mathbf{p}^2_{J/\Psi\,T}$.

$\mathbf{p}^2_{J/\Psi\,T}$ integration limits are taken as given by inelastic $J/\Psi$ process requirements: $1\,\mathrm{GeV}^2 \leq \mathbf{p}^2_{J/\Psi\,T} \leq s/4 - m^2_{J/\Psi}$. According to (1) the $\mathbf{q}^2_{2T}$ integration region was divided into two parts: $0 < \mathbf{q}^2_{2T} \leq Q^2_0$ and $\mathbf{q}^2_{2T} \geq Q^2_0$. The calculations are made according to (10) for $\mathbf{q}^2_{2T} \geq Q^2_0$ and for $0 < \mathbf{q}^2_{2T} \leq Q^2_0$ we use $\sum |M|^2_{\mathrm{PM}}(e\,g \to e'\,J/\Psi\,g')$ instead of $\sum |M|^2_{\mathrm{SHA}}(e\,g^* \to e'\,J/\Psi\,g')$ (see also (12)). The choice of the critical value of parameter $Q^2_0 = 1\,\mathrm{GeV}^2$ is determined by the requirement that the value of $\alpha_S(\mathbf{q}^2_{2T})$ be small in the region $\mathbf{q}^2_{2T} \geq 1\,\mathrm{GeV}^2$, where in fact $\alpha_S(\mathbf{q}^2_{2T}) \leq 0.26$.

The $Q^2$, $y_{J/\Psi}$ and $z$ integration limits are taken as given by kinematical conditions of H1 experimental data [42]. The first kinematical region is $2\,\mathrm{GeV}^2 \leq Q^2 \leq 80\,\mathrm{GeV}^2$, $40\,\mathrm{GeV} \leq W \leq 180\,\mathrm{GeV}$, $z > 0.2$, $M_X \geq 10\,\mathrm{GeV}$ and the second one is $\mathbf{p}^2_{J/\Psi\,T} \geq 4\,\mathrm{GeV}^2$, $4\,\mathrm{GeV}^2 \leq Q^2 \leq 80\,\mathrm{GeV}^2$, $40\,\mathrm{GeV} \leq W \leq 180\,\mathrm{GeV}$, $z > 0.2$, $M_X \geq 10\,\mathrm{GeV}$.

The results of our calculations are shown in Fig. 3—8. Fig. 3 show the $Q^2$-, $\mathbf{p}^2_{J/\Psi\,T}$-, $z$-, $y^*_{J/\Psi}$- and $W$-distributions of the inelastic $J/\Psi$ meson production obtained in the first kinematical region at $\sqrt{s} = 314\,\mathrm{GeV}$, $m_c = 1.55\,\mathrm{GeV}$ and $\Lambda_{\mathrm{QCD}} = 250\,\mathrm{MeV}$. Curve *1* corresponds to the SPM calculations at the leading order approximation with GRV gluon density, curves *2*, *3* and *4* correspond to the $k_T$-factorization results with JB, KMS and GBW unintegrated gluon distributions at $Q^2_0 = 1\,\mathrm{GeV}^2$. One can see that results obtained in the CS model with $k_T$-factorization (curves *2* — *4*) agree in shape but underestimate the H1 experimental data. The SPM calculation (curve *1*) are lower the data by a factor 2.

Fig. 4 show the $z$-, $y^*_{J/\Psi}$- and $W$-distributions of the inelastic $J/\Psi$ meson production obtained in the second kinematical region at $\sqrt{s} = 314\,\mathrm{GeV}$, $m_c = 1.55\,\mathrm{GeV}$ and $\Lambda_{\mathrm{QCD}} = 250\,\mathrm{MeV}$. Curves *1* — *4* are the same as in Fig. 3. One can see that in this kinematical region the $k_T$-factorization approach (curves *2* — *4*) describe the data better than in the first one (without cut $\mathbf{p}^2_{J/\Psi\,T} \geq 4\,\mathrm{GeV}^2$).

Fig. 5, 6 shows the $Q^2$-, $\mathbf{p}^2_{J/\Psi\,T}$-, $z$-, $y^*_{J/\Psi}$- and $W$-distributions of the inelastic $J/\Psi$ meson production at $\sqrt{s} = 314\,\mathrm{GeV}$, $m_c = 1.4\,\mathrm{GeV}$ and $\Lambda_{\mathrm{QCD}} = 250\,\mathrm{MeV}$ obtained in the first kinematical region (Fig. 5) and in the second one (Fig. 6). Curves *1* — *4* are the same as in Fig. 3. One can see that a shift the charm quark mass down to $m_c = 1.4\,\mathrm{GeV}$ increases the cross section by a factor 1.5, and results obtained in the CS model with $k_T$-factorization (curves *2* — *4*) agree with H1 experimental data.

The $z$-distributions are described at $z > 0.4$ only. It is because other $J/\Psi$ production mechanisms (such as resolved photon and/or colour octet contributions) may be impotant at $z < 0.4$ [60].

It is notable that the saturation unintegrated gluon distribution (GBW parametrization) does not contradict the HERA experimental data.

Fig. 3 — 6 show that $k_T$-factorization results with $m_c = 1.4\,\mathrm{GeV}$ (in contrast with SPM ones) for inelastic $J/\Psi$ electroproduction at HERA reasonably agree with H1 experimental data. Hovewer, at $m_c = 1.55\,\mathrm{GeV}$ some additional transition mechanism from $c\bar{c}$-pair to the $J/\Psi$ mesons (such as CO model) need for full description of these data.

We analyzed specially the influence of charm quark mass, $m_c$, on the our theoretical results. We found that the main effect of change of the charm quark mass connects with final phase space of $J/\Psi$ meson. In the subprocess matrix elements this effect is neglectable. However the value of $m_c = 1.4\,\mathrm{GeV}$ corresponds to the unphysical phase space of $J/\Psi$ state.[4)]

For studying $J/\Psi$ meson polarization properties we calculate the $\mathbf{p}^2_T$- and $Q^2$-dependences

[4)] We thank S. Baranov for the suggestion to study this problem.

of the spin aligment parameter $\alpha$ [19, 61] in the $k_T$-factorization approach and SPM:

$$\alpha(\omega) = \frac{d\sigma/d\omega - 3\,d\sigma_L/d\omega}{d\sigma/d\omega + d\sigma_L/d\omega}, \tag{25}$$

where $\sigma_L$ is the production cross section for the longitudinally polarized $J/\Psi$ mesons, $\omega = \mathbf{p}^2_{J/\Psi\,T}$, $Q^2$. The parameter $\alpha$ controls the angular distribution for leptons in the decay $J/\Psi \to \mu^+\,\mu^-$ (in the $J/\Psi$ meson rest frame):

$$\frac{d\Gamma(J/\Psi \to \mu^+\,\mu^-)}{d\cos\theta} \sim 1 + \alpha\,\cos^2\theta. \tag{26}$$

Fig. 7 shows the parameter $\alpha(\mathbf{p}_{J/\Psi\,T})$, which is calculated in the region $0.4 < z < 0.9$ (a) and in the region $0.4 < z < 1$ (b) at $\sqrt{s} = 314\,\mathrm{GeV}$, $m_c = 1.4\,\mathrm{GeV}$ and $\Lambda_{\mathrm{QCD}} = 250\,\mathrm{MeV}$ in comparison with preliminary experimental data taken by the ZEUS [43] collaboration at HERA. Curve *1* corresponds to the SPM calculations at the leading order approximation with GRV gluon density, curve *3* corresponds to the $k_T$-factorization QCD calculations with KMS unintegrated gluon distribution at $Q_0^2 = 1\,\mathrm{GeV}^2$.

We note that it is impossible to make of exact conclusions about a BFKL gluon contribution to the polarized $J/\Psi$ production cross section because of large incertainties in the experimental data and large additional contribution from initial longitudinal polarization of virtual photons. However at low $Q^2 < 1\,\mathrm{GeV}^2$ such contributions are neglected. This fact should result in observable spin effects of final $J/\Psi$ mesons. As example, we have performed calculations for the spin parameter $\alpha$ as a function $\mathbf{p}^2_{J/\Psi\,T}$ at fixed values of $Q^2$ for $40\,\mathrm{GeV} \le W \le 180\,\mathrm{GeV}$, $z > 0.2$, $M_X \ge 10\,\mathrm{GeV}$ at $\sqrt{s} = 314\,\mathrm{GeV}$, $m_c = 1.4\,\mathrm{GeV}$ and $\Lambda_{\mathrm{QCD}} = 250\,\mathrm{MeV}$.

The results of our calculations at fixed values of $Q^2 = 0.1\,\mathrm{GeV}^2$, $Q^2 = 1\,\mathrm{GeV}^2$, $Q^2 = 5\,\mathrm{GeV}^2$ and $Q^2 = 10\,\mathrm{GeV}^2$ are shown in Fig. 8. Curves *1* and *3* are the same as in Fig. 7. We have large difference between predictions of the leading order of SPM and the $k_T$-factorization approach at low $Q^2 < 1\,\mathrm{GeV}^2$, as it is seen in Fig. 8. Therefore if account of the NLO corrections (which is still unknown) will not change predictions of the LO SPM for $\alpha(\mathbf{p}^2_{J/\Psi\,T})$ at low $Q^2 < 1\,\mathrm{GeV}^2$, experimental measurement of polarization properties of the $J/\Psi$ mesons will be an additional test of BFKL gluon dynamics.

## 6 Conclusions

In this paper we considered $J/\Psi$ meson production in $ep$ deep inelastic scattering in the colour singlet model using the standart parton model at the leading order in $\alpha_S$ and the $k_T$-factorization QCD approach. We investigated the $z$-, $Q^2$-, $\mathbf{p}_T^2$-, $y^*$-, $W$-dependences of inelastic $J/\Psi$ production on different forms of the unintegrated gluon distribution. The $\mathbf{p}_T^2$- and $Q^2$-dependences of the spin aligment parameter $\alpha$ presented also. We compared the theoretical results with available experimental data taken by the H1 and ZEUS collaborations at HERA. We have found that the $k_T$-factorization results with JB, KMS and GBW unintegrated gluon distributions reasonably agree with H1 experimental data only at $m_c = 1.4\,\mathrm{GeV}$, $|\Psi(0)|^2 = 0.0876\,\mathrm{GeV}^3$ and $\Lambda_{\mathrm{QCD}} = 250\,\mathrm{MeV}$. At $m_c = 1.55\,\mathrm{GeV}$ some additional transition mechanism from $c\bar{c}$-pair to the $J/\Psi$ mesons (such as CO model) need for full description of these data. The saturation unintegrated gluon distribution (GBW parametrization) does

not contradict the existing experimental data. The experimental study of a polarization of $J/\Psi$ meson at low $Q^2 < 1\,\mathrm{GeV}^2$ should be additianal test of BFKL gluon dynamics.

The authors would like to thank S. Baranov for encouraging interest and useful discussions. A.L. thanks also V. Saleev for the help on the initial stage of work. The study was supported in part by RFBR grant 02–02–17513.

## References

[1] E.L. Berger and D. Jones, Phys. Rev. D **23**, 1521 (1981).

[2] S.S. Gershtein, A.K. Likhoded, S.R. Slabospitsky, Sov. J. Nucl. Phys. **34**, 128 (1981).

[3] R. Baier, R. Ruckl, Nucl. Phys. B **218**, 289 (1983).

[4] A.D. Martin, C.K. Ng, W.J. Stirling, Phys. Lett. B **191**, 200 (1987).

[5] L. Gribov, E. Levin, M. Ryskin, Phys. Rep. **100**, 1 (1983).

[6] E.M. Levin, M.G. Ryskin, Yu.M. Shabelsky, A.G. Shuvaev, Sov. J. Nucl. Phys. **53**, 657 (1991).

[7] S. Catani, M. Ciafoloni, F. Hautmann, Nucl. Phys. B **366**, 135 (1991).

[8] J.C. Collins, R.K. Ellis, Nucl. Phys. B **360**, 3 (1991).

[9] E. Kuraev, L. Lipatov, V. Fadin, Sov. Phys. JETP **44**, (1976) 443;
E. Kuraev, L. Lipatov, V. Fadin, Sov. Phys. JETP **45**, (1977) 199;
Yu. Balitsky, L. Lipatov, Sov. J. Nucl. Phys. **28**, (1978) 822.

[10] B. Andersson *et al.* (The Small $x$ Collab.), DESY 02-041; hep-ph/0204115.

[11] M.G. Ryskin, Yu.M. Shabelski, Z. Phys. C **69**, 269 (1996).

[12] M.G. Ryskin, Yu.M. Shabelski, Z. Phys. C **61**, 517 (1994);
Z. Phys. C **66**, 151 (1995).

[13] V.A. Saleev, N.P. Zotov, Mod. Phys. Lett. A **9**, 151 (1994).

[14] V.A. Saleev, N.P. Zotov, Mod. Phys. Lett. A **11**, 25 (1996).

[15] A.V. Lipatov, N.P. Zotov, Mod. Phys. Lett. A **15**, 695 (2000).

[16] A.V. Lipatov, V.A. Saleev, N.P. Zotov, Mod. Phys. Lett. A **15**, 1727 (2000).

[17] A.V. Lipatov, N.P. Zotov, in *Proceedings of the 8th International Workshop on DIS and QCD*, DIS'2000 (Liverpool, 2000), p.157.

[18] A.V. Kotikov, A.V. Lipatov, G. Parente, N.P. Zotov, hep-ph/0107135.

[19] S.P. Baranov, Phys. Lett. B **428**, 377 (1998).

[20] S.P. Baranov, N.P. Zotov, Phys. Lett. B **458**, 389 (1999);
S.P. Baranov, N.P. Zotov, Phys. Lett. B **491**, 111 (2000).

[21] S.P. Baranov, M. Smizanska, Phys. Rev. D **62**, 014012 (2000).

[22] P. Hagler, R. Kirschner, A. Schefer *et al.*, Phys. Rev. D **62**, 071502 (2000).

[23] H. Jung, Phys. Rev. D **65**, 034015 (2002); hep-ph/0110034.

[24] P. Hagler, R. Kirschner, A. Schefer *et al.*, Phys. Rev. D **63**, 077501 (2001);
F. Yuan, K.-T. Chao, Phys. Rev. D **63**, 034006 (2001); hep-ph/0009224.

[25] H. Jung, hep-ph/0110345.

[26] E. Braaten, S. Fleming, Phys. Rev. Lett. **74**, 3327 (1995);
E. Braaten, T.C. Yuan, Phys. Rev. D **52**, 6627 (1995).

[27] P. Cho, A.K. Leibovich, Phys. Rev. D **53**, 150 (1996);
P. Cho, A.K. Leibovich, Phys. Rev. **53**, 6203 (1996).

[28] G.T. Bodwin, E. Braaten, G.P. Lepage, Phys. Rev. D **51**, 1125 (1995);
G.T. Bodwin, E. Braaten, G.P. Lepage, Phys. Rev. D **55**, 5853 (1997).

[29] M. Cacciari, M. Kramer, Phys. Rev. Lett. **76**, 4128 (1996).

[30] P. Ko, J. Lee, H.S. Song, Phys. Rev. D **54**, 4312 (1996);
P. Ko, J. Lee, H.S. Song, Phys. Rev. D **60**, 119902 (1999).

[31] S. Aid *et al.* (H1 Collab.), Nucl. Phys. B **472**, 3 (1996).

[32] J. Breitweg *et al.* (ZEUS Collab.), Z. Phys. C **96**, 599 (1997).

[33] S. Fleming, T. Mehen, Phys. Rev. D **57**, 1846 (1998).

[34] B.A. Kniehl, L. Zwirner, hep-ph/0112199.

[35] J.C. Korner, J. Cleymans, M. Kuroda, G.J. Gounaris, Phys. Lett. B **114**, 195 (1982).

[36] J.-Ph. Guillet, Z. Phys. C **39**, 75 (1988).

[37] H. Merabet, J.F. Mathiot, R. Mendez-Galain, Z. Phys. C **62**, 639 (1994).

[38] F. Yuan, K.-T. Chao, Phys. Rev. D **63**, 034017 (2001).

[39] F. Yuan, K.-T. Chao, Phys. Rev. Lett. D **87**, 022002-L (2001).

[40] Ph. Hagler *et al.*, Phys. Rev. Lett. **86**, 1446 (2001).

[41] B. Guberina *et al.*, Nucl. Phys. B **174**, 317 (1980).

[42] C. Adloff *et al.* (H1 Collab.), DESY-99-026.

[43] R. Brugnera, (ZEUS Collab.), in *Proceedings of the 9th International Workshop on DIS and QCD*, DIS'2001 (Bologna, Italy, 2001).

[44] J. Blumlein, DESY 95-121.

[45] M. Gluck, E. Reya, A. Vogt, Z. Phys. C **67**, 433 (1995).

[46] V. Fadin, L. Lipatov, Phys. Lett. B **429**, 127 (1998);
M. Ciafaloni, G. Camici, Phys. Lett. B **430**, 349 (1998).

[47] G. Salam, JHEP, **9807:019**, (1998); hep-ph/9806482.

[48] S.J. Brodsky, V.S. Fadin, V.T. Kim, L.N. Lipatov, G.B. Pivovarov, hep-ph/9901229.

[49] J. Kwiecinski, A. Martin, A. Stasto, Phys. Rev. D **56**, 3991 (1997).

[50] J. Kwiecinski, A. Martin, A. Sutton, Phys. Rev. D **52**, 1445 (1995);
Z. Phys. C **71**, 585 (1996).

[51] J. Kwiecinski, A. Martin, J. Outhwaite, Eur. Phys. J. C **9**, 611 (2001);

[52] K. Colec-Biernat, M. Wusthoff, Phys. Rev. D **59**, 014017 (1999).

[53] K. Colec-Biernat, M. Wusthoff, Phys. Rev. D **60**, 114023 (1999).

[54] M. Beneke, M. Kramer, Phys. Rev. D **55**, 5269 (1997).

[55] M. Kramer, Nucl. Phys. B **459**, 3 (1996).

[56] S. Narison, Phys. Lett. B **341**, 73 (1994).

[57] P. Ball, M. Beneke, V. Braun, Phys. Rev. D **52**, 3929 (1995).

[58] E.M. Levin, M.G. Ryskin, Yu.M. Shabelsky, A.G. Shuvaev, Yad. Fiz. **54**, 1420 (1991).

[59] A.V. Lipatov, *Talk at International School "Heavy Quark Physics"*, HQP'2002 (Dubna, Russia, 27 May — 5 June, 2002);
N.P. Zotov, *Talk at "Small x collaboration" meeting* (Lund, Sweden, 5 — 6 June, 2002).

[60] H1 Collab., *International Eur. Phys. Conference on High Energy Physics*, HEP'99 (Tampere, Finland, 1996).

[61] S.P. Baranov, A.V. Lipatov, N.P. Zotov, in *Proceedings of the 9th International Workshop on DIS and QCD*, DIS'2001 (Bologna, Italy, 2001), hep-ph/0106229.

**Fig. 1.** Diagram for $e\,p \to e'\,J/\Psi\,X$ process.

**Fig. 2.** Feynmans diagram used for description partonic process $\gamma\,g \to J/\Psi\,g'$ process.

**Fig. 3.** The $Q^2$-, $\mathbf{p}^2_{J/\Psi\,T}$-, $z$-, $y^*_{J/\Psi}$- and $W$-distributions of the inelastic $J/\Psi$ production obtained in the kinematical region $2\,\mathrm{GeV}^2 \le Q^2 \le 80\,\mathrm{GeV}^2$, $40\,\mathrm{GeV} \le W \le 180\,\mathrm{GeV}$, $z > 0.2$, $M_X \ge 10\,\mathrm{GeV}$ at $\sqrt{s} = 314\,\mathrm{GeV}$, $m_c = 1.55\,\mathrm{GeV}$ and $\Lambda_{\mathrm{QCD}} = 250\,\mathrm{MeV}$. Curve *1* corresponds to the SPM calculations at the leading order approximation with GRV gluon density, curves *2*, *3* and *4* correspond to the $k_T$-factorization QCD calculations with JB, KMS and GBW unintegrated gluon distribution at $Q_0^2 = 1\,\mathrm{GeV}^2$.

**Fig. 4.** The $z$-, $y^*_{J/\Psi}$- and $W$-distributions of the inelastic $J/\Psi$ production obtained in the kinematical region $\mathbf{p}^2_{J/\Psi\,T} \ge 4\,\mathrm{GeV}^2$, $4\,\mathrm{GeV}^2 \le Q^2 \le 80\,\mathrm{GeV}^2$, $40\,\mathrm{GeV} \le W \le 180\,\mathrm{GeV}$, $z > 0.2$, $M_X \ge 10\,\mathrm{GeV}$ at $\sqrt{s} = 314\,\mathrm{GeV}$, $m_c = 1.55\,\mathrm{GeV}$ and $\Lambda_{\mathrm{QCD}} = 250\,\mathrm{MeV}$. Curves *1* — *4* are the same as in Fig. 3.

**Fig. 5.** The $Q^2$-, $\mathbf{p}^2_{J/\Psi\,T}$-, $z$-, $y^*_{J/\Psi}$- and $W$-distributions of the inelastic $J/\Psi$ production obtained in the kinematical region $2\,\mathrm{GeV}^2 \le Q^2 \le 80\,\mathrm{GeV}^2$, $40\,\mathrm{GeV} \le W \le 180\,\mathrm{GeV}$, $z > 0.2$, $M_X \ge 10\,\mathrm{GeV}$ at $\sqrt{s} = 314\,\mathrm{GeV}$, $m_c = 1.4\,\mathrm{GeV}$ and $\Lambda_{\mathrm{QCD}} = 250\,\mathrm{MeV}$. Curves *1* — *4* are the same as in Fig. 3.

**Fig. 6.** The $z$-, $y^*_{J/\Psi}$- and $W$-distributions of the inelastic $J/\Psi$ production obtained in the kinematical region $\mathbf{p}^2_{J/\Psi\,T} \ge 4\,\mathrm{GeV}^2$, $4\,\mathrm{GeV}^2 \le Q^2 \le 80\,\mathrm{GeV}^2$, $40\,\mathrm{GeV} \le W \le 180\,\mathrm{GeV}$, $z > 0.2$, $M_X \ge 10\,\mathrm{GeV}$ at $\sqrt{s} = 314\,\mathrm{GeV}$, $m_c = 1.4\,\mathrm{GeV}$ and $\Lambda_{\mathrm{QCD}} = 250\,\mathrm{MeV}$. Curves *1* — *4* are the same as in Fig. 3.

**Fig. 7.** The parameter $\alpha(\mathbf{p}_{J/\Psi\,T})$, which is calculated in the region $0.4 < z < 0.9$ (a) and in the region $0.4 < z < 1$ (b) at $\sqrt{s} = 314\,\mathrm{GeV}$, $m_c = 1.4\,\mathrm{GeV}$ and $\Lambda_{\mathrm{QCD}} = 250\,\mathrm{MeV}$. Curve *1* corresponds to the SPM calculations at the leading order approximation with GRV gluon density, curve *3* corresponds to the $k_T$-factorization QCD calculations with KMS unintegrated gluon distribution at $Q_0^2 = 1\,\mathrm{GeV}^2$.

**Fig. 8.** The spin aligment parameter $\alpha(\mathbf{p}^2_{J/\Psi\,T})$ at fixed values of $Q^2$ for $40\,\mathrm{GeV} \le W \le 180\,\mathrm{GeV}$, $z > 0.2$, $M_X \ge 10\,\mathrm{GeV}$ at $\sqrt{s} = 314\,\mathrm{GeV}$, $m_c = 1.4\,\mathrm{GeV}$ and $\Lambda_{\mathrm{QCD}} = 250\,\mathrm{MeV}$. Curves *1* and *3* are the same as in Fig. 7.

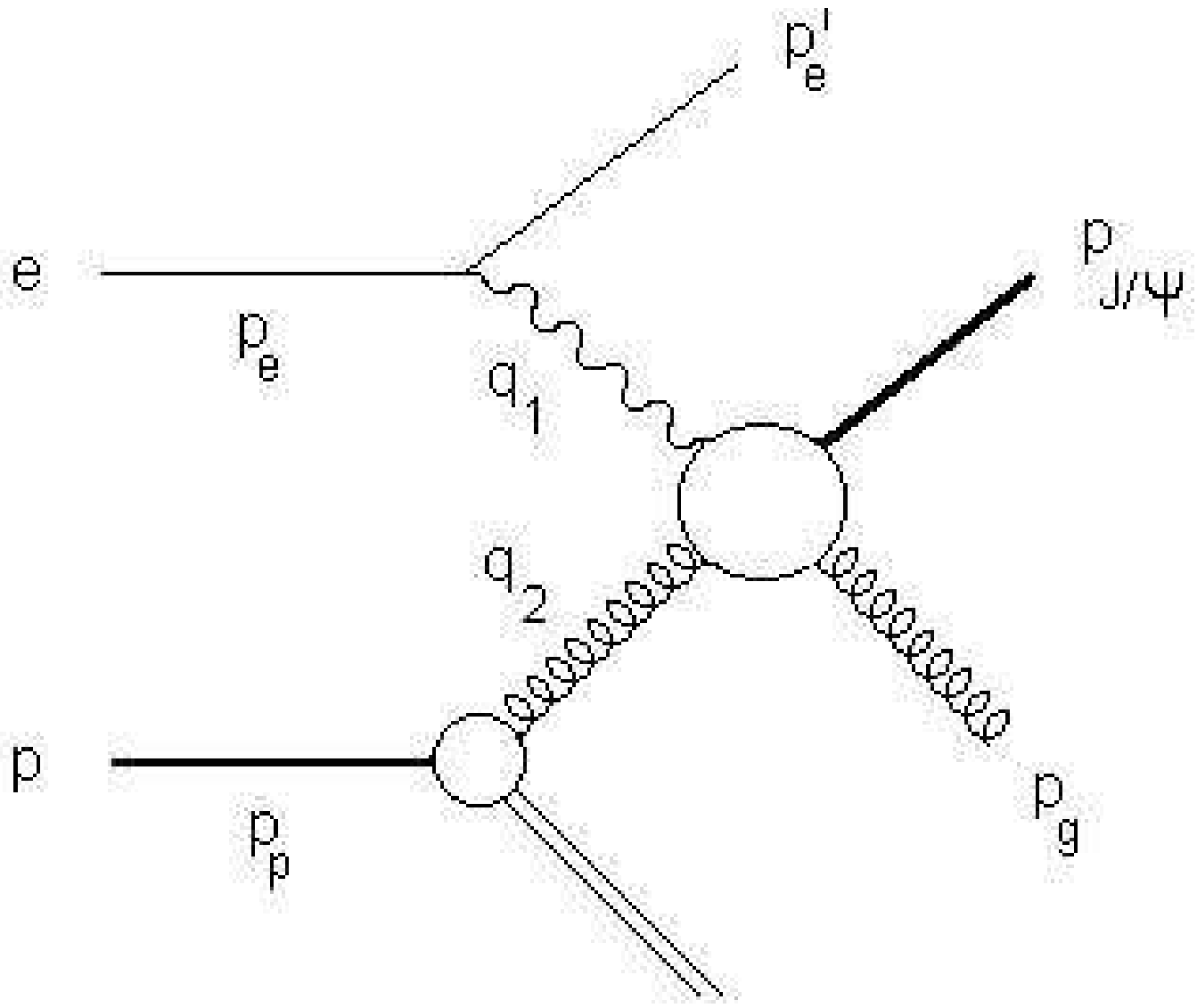
p'e
e
pe
q1
pJ/ψ
q2
p
pp
pg

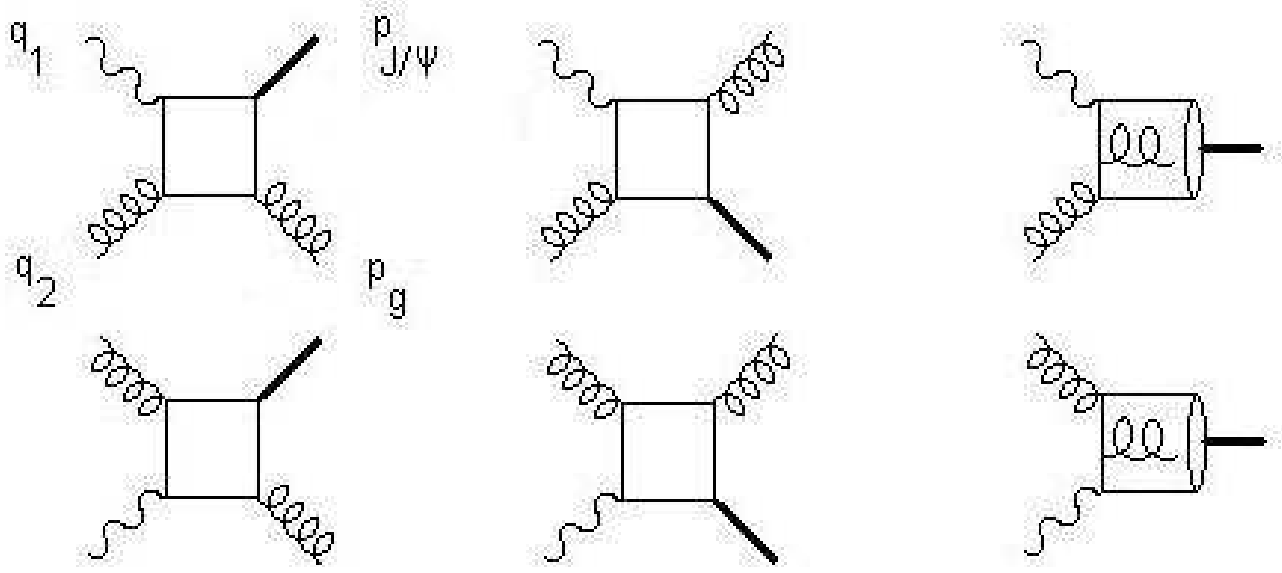
q1
q2
pJ/ψ
pg
QQ
QQ

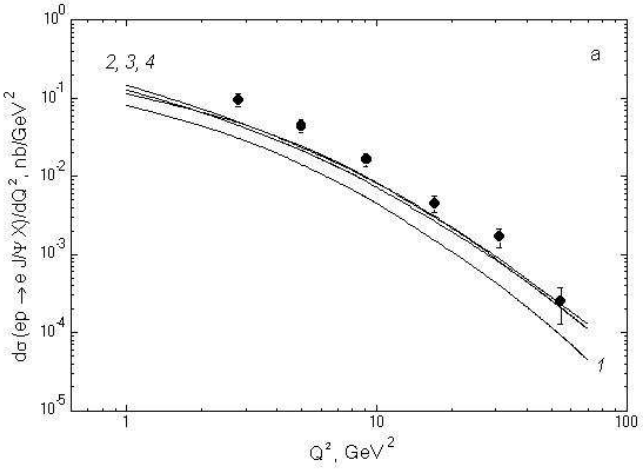
a
2, 3, 4
1
dσ (ep → e J/Ψ X)/dQ², nb/GeV²
Q², GeV²

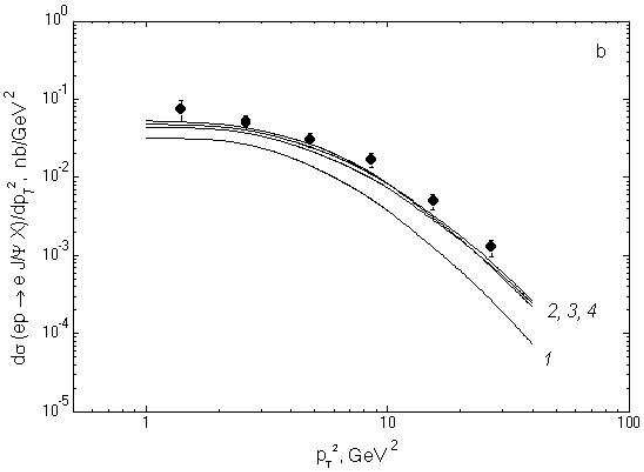
b
2, 3, 4
1
dσ (ep → e J/Ψ X)/dp_T², nb/GeV²
p_T², GeV²

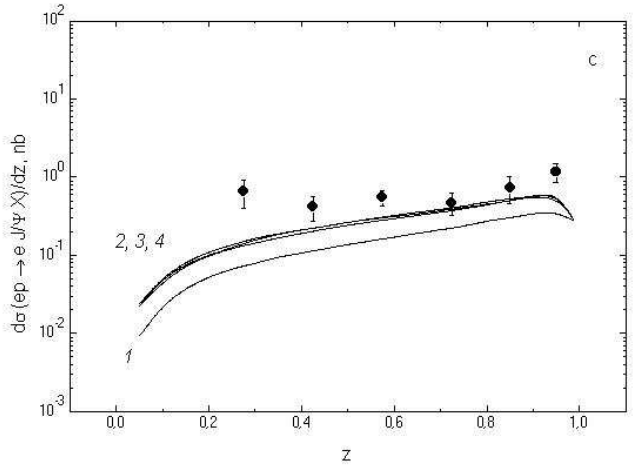
c
2, 3, 4
1
dσ (ep → e J/Ψ X)/dz, nb
z

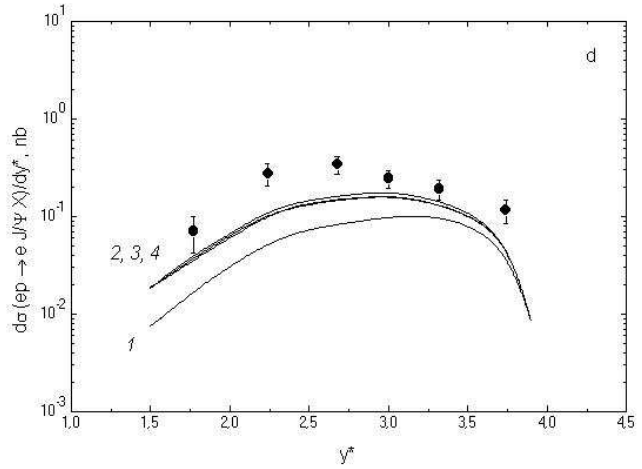
d
2, 3, 4
1
dσ (ep → e J/Ψ X)/dy*, nb
y*

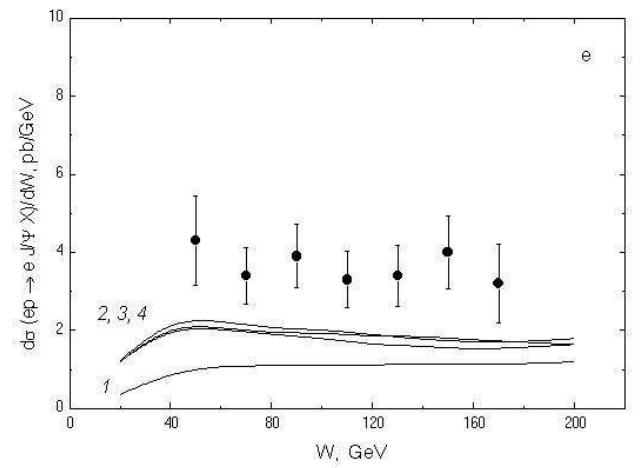
e
2, 3, 4
1
dσ (ep → e J/Ψ X)/dW, pb/GeV
W, GeV

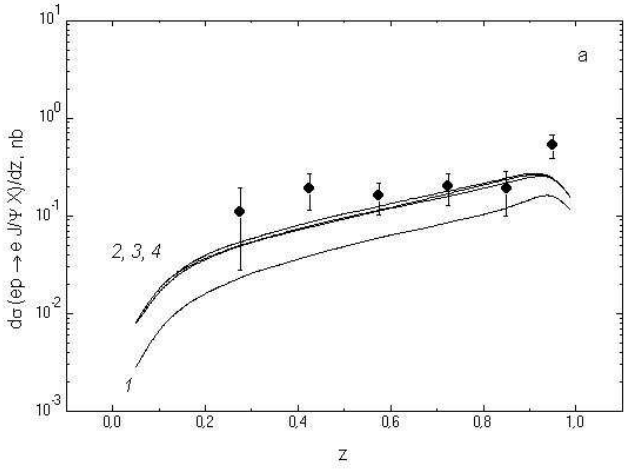
a
2, 3, 4
1
dσ (ep → e J/Ψ X)/dz, nb
z

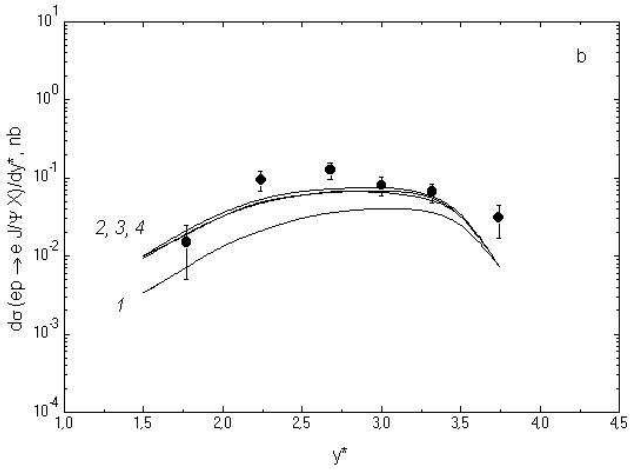
b
2, 3, 4
1
dσ (ep → e J/Ψ X)/dy*, nb
y*

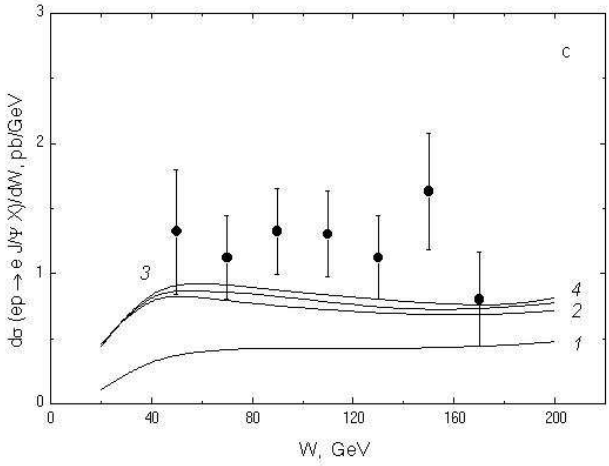
c
3
4
2
1
dσ (ep → e J/Ψ X)/dW, pb/GeV
W, GeV

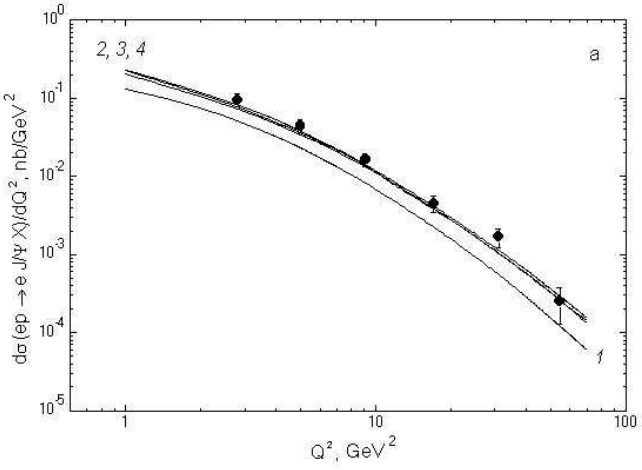
a
2, 3, 4
1
dσ (ep → e J/Ψ X)/dQ², nb/GeV²
Q², GeV²

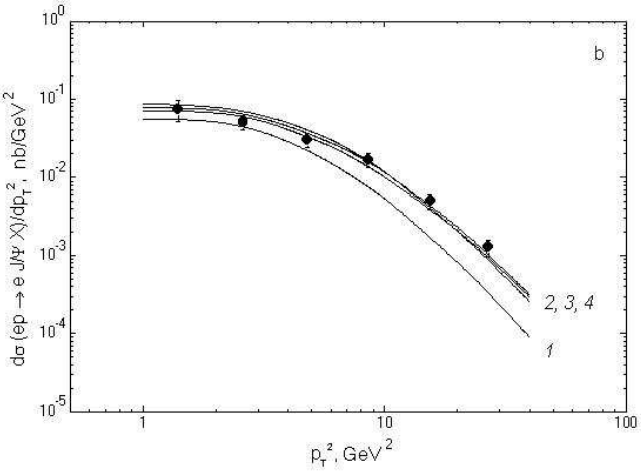
b
2, 3, 4
1
dσ (ep → e J/Ψ X)/dp_T², nb/GeV²
p_T², GeV²

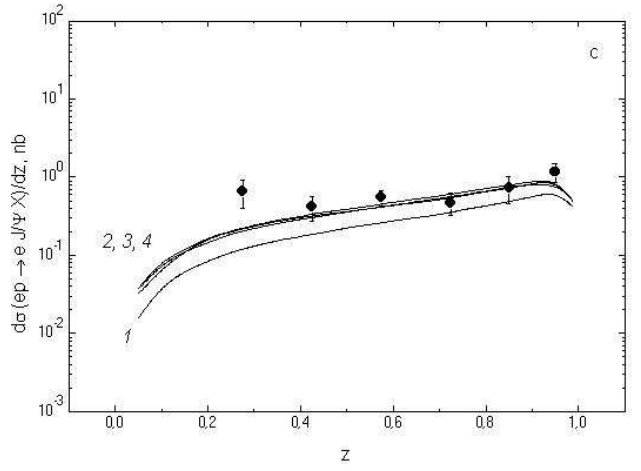
c
2, 3, 4
1
dσ (ep → e J/Ψ X)/dz, nb
z

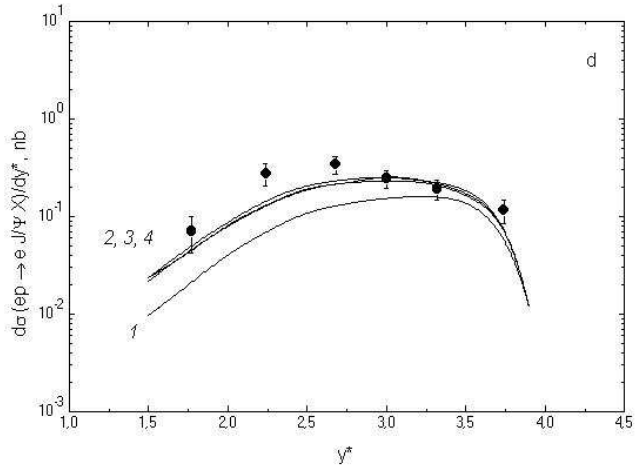
d
2, 3, 4
1
dσ (ep → e J/Ψ X)/dy*, nb
y*

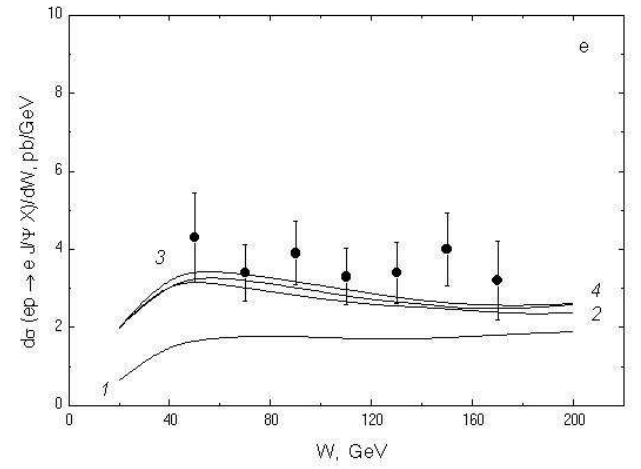
e
3
4
2
1
dσ (ep → e J/Ψ X)/dW, pb/GeV
W, GeV

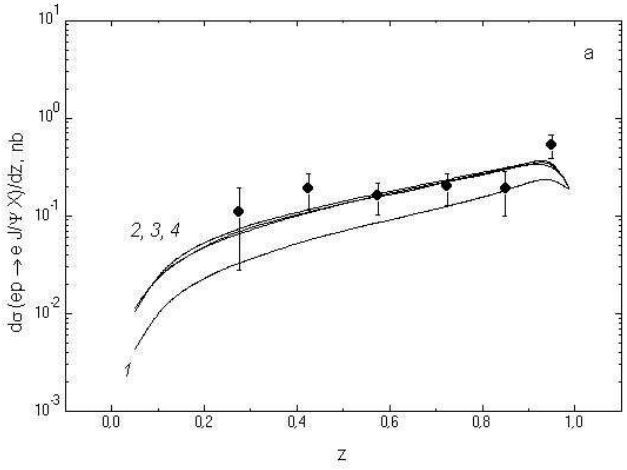
a
2, 3, 4
1
dσ(ep → e J/Ψ X)/dz, nb
z

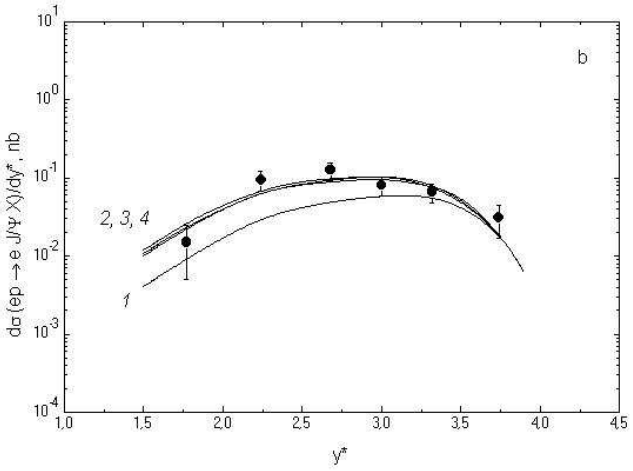
b
2, 3, 4
1
dσ(ep → e J/Ψ X)/dy*, nb
y*

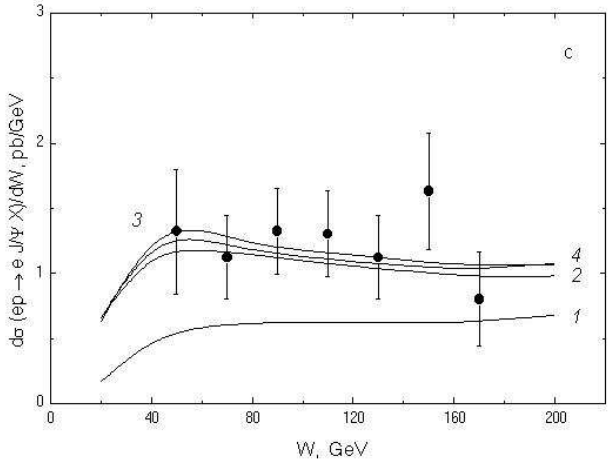
c
3
4
2
1
dσ(ep → e J/Ψ X)/dW, pb/GeV
W, GeV

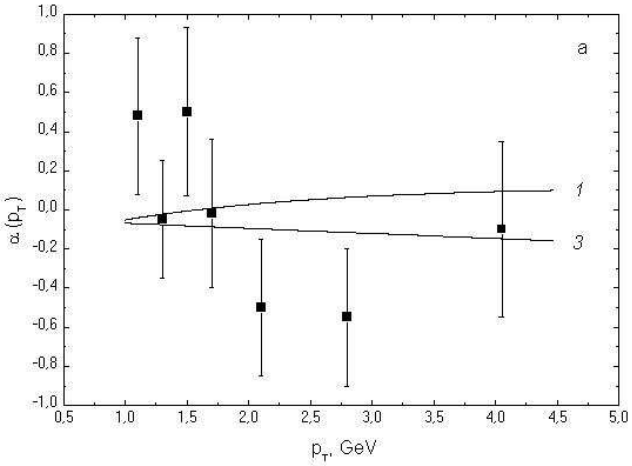
a
1
3
α (p_T)
p_T, GeV

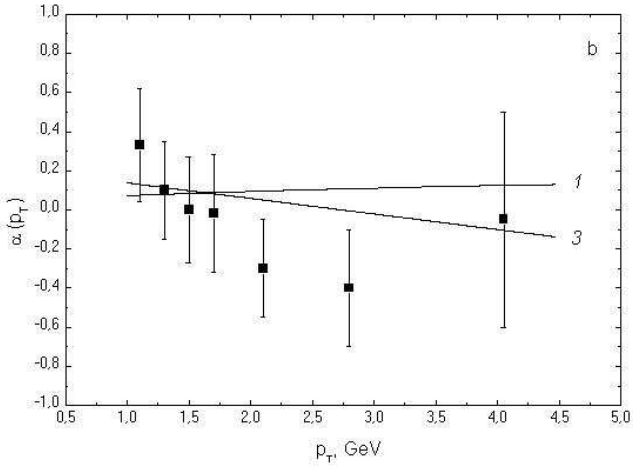
b
1
3
α (p_T)
p_T, GeV

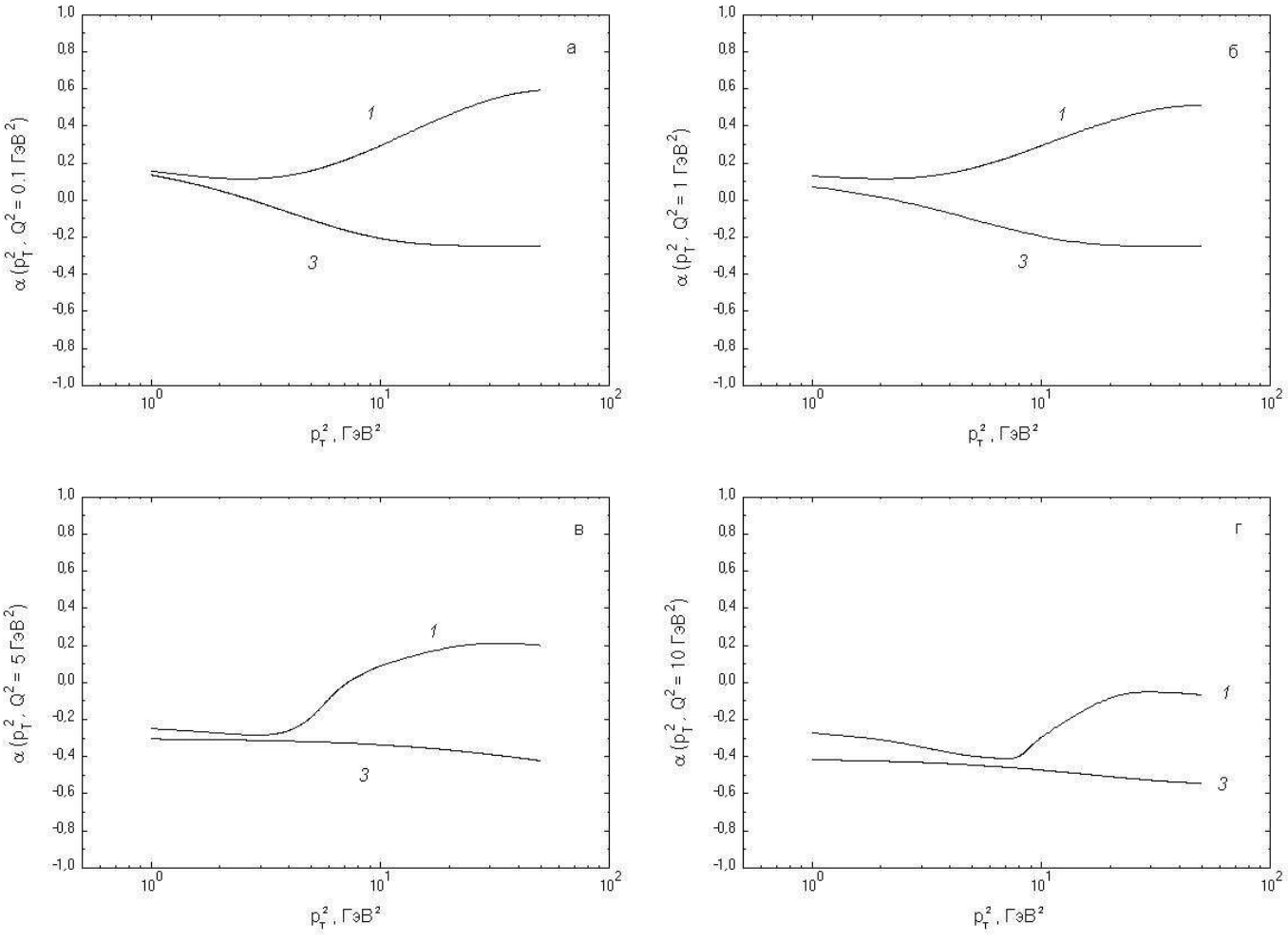
а
б
в
г
1
3
$\alpha(p_T^2, Q^2 = 0.1\ ГэВ^2)$
$\alpha(p_T^2, Q^2 = 1\ ГэВ^2)$
$\alpha(p_T^2, Q^2 = 5\ ГэВ^2)$
$\alpha(p_T^2, Q^2 = 10\ ГэВ^2)$
$p_T^2$, $ГэВ^2$
1,0
0,8
0,6
0,4
0,2
0,0
-0,2
-0,4
-0,6
-0,8
-1,0
$10^0$
$10^1$
$10^2$